

Comparison on Vector Magnetometer Configuration Schemes in Magnetic Localization Experiment

Yu Huang^{1,2}, Yanling Hao²

¹ School of Science, Harbin Engineering University, Harbin 150001, China
Email: huangyu_cge@china.com.cn

² School of Automatic, Harbin Engineering University, Harbin 150001, China
Email: YLhao@sina.com.cn

Abstract— Two kinds of configuration schemes about eight and ten single-axis vector magnetometers are put forward on the basis of describing the principle of underwater magnetic field localization. The measurement equations of magnetic field magnitude and gradients are deduced on condition of two configuration schemes, and that the calculated precisions of both magnetic field magnitude and gradients are compared and analyzed. The relationships between the length of measurement baseline ΔX and the errors of magnetic field magnitude, gradients and vehicle position relative to target are simulated numerically, and that the results show that these errors will increase when ΔX is lengthened. The calculated precisions of both magnetic field magnitude and gradients on condition of ten single-axis vector magnetometers are both largely higher than that on condition of eight ones, and things are the same for the localization precision of underwater vehicle. So, the ten single-axis vector magnetometers configuration should be selected in the magnetic field localization experiment of underwater vehicle.

Index Terms—magnetic field localization, magnetic field gradient, magnetometer, configuration scheme

I. INTRODUCTION

Geomagnetic aided navigation is a novel passive navigation method aroused at the end of the twentieth century, whose navigation precision can be achieved to be very high, and its applications about small satellite orbit determination and missile guidance have been reported [1-4]. Because geomagnetic aided navigation belongs to navigation method based on transcendental maps, its navigation precision would be affected by mapping accuracy of transcendental maps. However, the effective geomagnetic maps are usually surveyed and mapped on the marine surface or in the air, and they can only describe the geomagnetic field on the surveying and mapping surfaces, but can't describe the geomagnetic anomaly produced by geologic structural changes and ferromagnetic object [5-6]. Your goal is to simulate the usual appearance of papers in a Conference Proceedings of the Academy Publisher. We are requesting that you follow these guidelines as closely as possible.

In order to automatic geomagnetic localization under water, a solution based on magnetic anomaly is put forward: the magnetic anomaly is inversed a magnetic dipole target and the position of underwater vehicle relative to the target is determined by measuring magnetic field magnitude and gradient of the target, and then the exact position of the vehicle is achieved by SLAM (simultaneous location and mapping) algorithm [7-9]. So, a lot of magnetometers installed on the vehicle are used to measure magnetic field magnitude and gradient of the target. In this text, two kinds of configuration schemes about eight and ten single-axis vector magnetometers are put forward and compared, and the measurement equations of magnetic field magnitude and gradient are deduced on condition of two configuration schemes. Both the calculated precision about magnetic field of the target and localization precision of vehicle are compared and analyzed in these kinds of configuration schemes. It is important for the researchers to select the configuration scheme about vectors magnetometers reasonably in the experiment of underwater vehicle magnetic localization.

II. PRINCIPLE OF UNDERWATER MAGNETIC FIELD LOCALIZATION

The underwater magnetic target comes from geomagnetic anomaly and ferromagnetic object, whose magnetic field is only several hundred nano-Tesla or less, which is less than earth magnetic background field by several magnitudes. The target can be treated as a magnetic dipole when the measuring point $P(X, Y, Z)$ is far away from it, which can be described by six unknown quantities such as three-dimension position parameters and magnetic moment (m_x, m_y, m_z). The parameter t represents the magnetic field magnitude of the target in the measuring point P , and its five independent magnetic field gradient components are respectively chosen as $a=g_{xx}=\partial B_x/\partial X$, $b=g_{yy}=\partial B_y/\partial Y$, $d=g_{yx}=\partial B_y/\partial X$, $e=g_{zy}=\partial B_z/\partial Y$ and $f=g_{zx}=\partial B_z/\partial X$, B_x, B_y, B_z represent the X, Y and Z components of magnetic induction intensity of the point P respectively. Combined with the harmonic field property excited by magnetic dipole, the magnetic moments m_x, m_y and m_z can be eliminated, and then the

Corresponding author. Tel: +(086-0451-82519465); fax: +(086-

vehicle position parameters X, Y, Z relative to the target are calculated, respectively [9]

$$Z = \pm 3t[(akq+dq+f)^2 + (dkq+bq+e)^2 + (fkq+eq+c)^2]^{-1/2} \quad (1a)$$

$$X = kqZ \quad (1b)$$

$$Y = qZ \quad (1c)$$

where, $c = g_{ZZ} = \partial B_Z / \partial Z = -(a+b)$, $q = [d(k^2-1) - (a-b)k] / [(ek-f)(k^2+1)]$, and k is a parameter determined by a six order equation with one variable as follows

$$A_6 k^6 + A_5 k^5 + A_4 k^4 + A_3 k^3 + A_2 k^2 + A_1 k + A_0 = 0 \quad (2)$$

where, the coefficients A_i ($i=0, 1, \dots, 6$) of the six order equation are $A_6 = d^2(a+2b) - e^2(a-b) + 2def$,

$$A_5 = -2d[(a-b)(a+2b) + d^2 + e^2 + f^2],$$

$$A_4 = (a-b)^2(a+2b) + d^2(4a-7b) - (2e^2 - f^2)(a-b) + 6def,$$

$$A_3 = -4d[(a-b)^2 - d^2 + e^2 + f^2],$$

$$A_2 = (a-b)^2(a+2b) - d^2(7a-4b) - (e^2 - f^2)(a-b) + 6def, A_1 = -A_5,$$

$$A_0 = d^2(2a+b) + f^2(a-b) + 2def, \text{ respectively.}$$

III. TWO KINDS OF CONFIGURATION SCHEMES AND THEIR MEASURING EQUATIONS

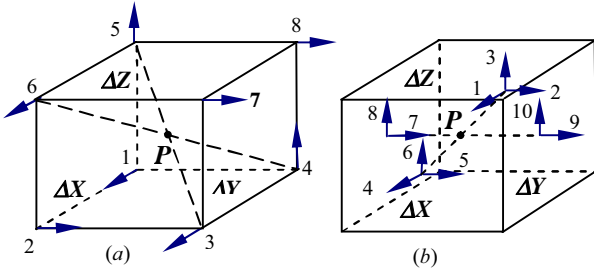


Fig.1 Two magnetometers configuration sketches

The configuration scheme with eight and ten single-axis magnetometers is shown in Fig.1(a) and (b), and the point P lies in the center of cuboid. In Fig.(a), magnetometers are respectively installed on the vertexes of a cuboid, whose length, width and height are respectively $\Delta X, \Delta Y$ and ΔZ . In Fig.(b), magnetometer team with X sensitive axis (1, 2, 3) and (4, 5, 6), team with Y sensitive axis (7, 8) and (9, 10) are placed around P symmetrically along with X and Y direction.

The measurement equations of magnetic field gradient and magnitude in eight magnetometers configuration are shown in Equ.(3a) and (3b), respectively.

$$g^{(1)} = HB^{(1)} \quad (3a)$$

$$t^{(1)} = [(B_1+B_3+B_6)^2/9 + (B_2+B_7+B_8)^2/9 + (B_4+B_5)^2/4]^{1/2} \quad (3b)$$

where, $g^{(1)T} = [a^{(1)}, b^{(1)}, d^{(1)}, e^{(1)}, f^{(1)}]$ and $B^{(1)T} = [B_1, B_2, B_3, B_4, B_5, B_6, B_7, B_8]$ are the vectors of magnetic field gradients and components measured by eight magnetometers, respectively, and the symbol T means transpose operation. $H = [H_{ij}]$ ($i=1,2, \dots,5; j=1,2, \dots,8$) is measurement matrix of magnetic field gradient in this eight magnetometers configuration, whose elements are $H_{11} = -H_{13} = -1/\Delta X, H_{12} = H_{14} = H_{15} = H_{16} = 0, H_{17} = -H_{18} = -\Delta Y/\Delta X^2, H_{21} = -H_{23} = \Delta Z^2/[\Delta X(\Delta Z^2 - \Delta Y^2)], H_{22} = \Delta Y/(\Delta Z^2 - \Delta Y^2), H_{24} = -H_{25} = \Delta Z/(\Delta Z^2 - \Delta Y^2), H_{26} = 0, H_{27} = (\Delta Z^2 - \Delta X^2)\Delta Y/[\Delta X^2(\Delta Z^2 - \Delta Y^2)], H_{28} = -\Delta Y\Delta Z^2/[\Delta X^2(\Delta Z^2 - \Delta Y^2)]; H_{31} = H_{32} = H_{33} = H_{34} = H_{35} = H_{36} = 0, H_{37} = -H_{38} = 1/\Delta X; H_{41} = -H_{43} = \Delta Y\Delta Z/[\Delta X(\Delta Y^2 - \Delta Z^2)], H_{42} = \Delta Z/(\Delta Y^2 - \Delta Z^2), H_{44} = -H_{45} = \Delta Y/(\Delta Y^2 - \Delta Z^2), H_{46} = 0,$

$$H_{47} = (\Delta Y^2 - \Delta X^2)\Delta Z/[\Delta X^2(\Delta Y^2 - \Delta Z^2)],$$

$$H_{48} = -\Delta Y^2\Delta Z/[\Delta X^2(\Delta Y^2 - \Delta Z^2)]; H_{51} = H_{52} = H_{54} = H_{55} = 0,$$

$$H_{53} = -H_{56} = -1/\Delta Z, H_{57} = -H_{58} = \Delta Y/(\Delta X\Delta Z).$$

The measurement equations of magnetic field gradient and magnitude in ten magnetometers configuration are shown in Equ.(4a) and (4b), respectively.

$$g^{(2)} = CB^{(2)} \quad (4a)$$

$$t^{(2)} = [4(B_1+B_4)^2 + (B_2+B_5+B_7+B_9)^2 + (B_3+B_6+B_8+B_{10})^2]^{1/2}/4 \quad (4b)$$

where, $g^{(2)T} = [a^{(2)}, b^{(2)}, d^{(2)}, e^{(2)}, f^{(2)}]$ and $B^{(2)T} = [B_1, B_2, B_3, B_4, B_5, B_6, B_7, B_8, B_9, B_{10}]$ are the vectors of magnetic field gradient and components measured by ten magnetometers, respectively, and C is measurement matrix of magnetic field gradient in ten magnetometers configuration whose elements are $C_{11} = C_{32} = C_{53} = -C_{14} = -C_{35} = C_{56} = -1/\Delta X, C_{27} = C_{48} = -C_{29} = C_{4,10} = -1/\Delta Y$, and others are all zeros.

IV. SIMULATIONS AND DISCUSSION

The simulation parameters are: the magnetic dipole target is located on the origin of space coordinate system, whose three components of magnetic moment are $m_X = 100A \cdot m^2, m_Y = 20A \cdot m^2$ and $m_Z = 10A \cdot m^2$, respectively. The center of device measuring magnetic field gradient is located on P , whose positions in the X, Y and Z directions are $X_s = 100m, Y_s = 50m$ and $Z_s = 30m$, respectively. The measurement lines are selected as $\Delta X = \Delta Y = 2\Delta Z$ and $\Delta X = \Delta Y$ in eight and ten magnetometers configuration schemes, respectively.

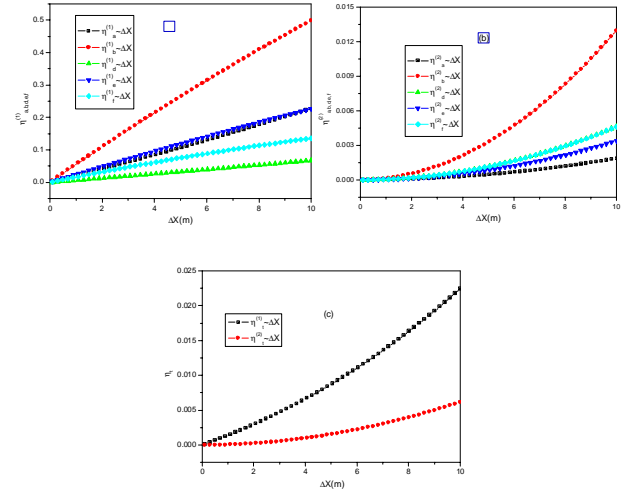


Fig.2 Curves between the relative error of magnetic field gradient and magnitude and ΔX

The symbols $t_s, a_s, b_s, d_s, e_s, f_s$ are respectively the theoretical values of magnetic field magnitude and gradients in the point $P. \eta^{(i)}_t = |(t^{(i)} - t_s)/t_s|$ ($i=1,2$) represent the relative error of magnetic field magnitude in eight and ten single-axis magnetometers configuration schemes, respectively. $\eta^{(i)}_a = |(a^{(i)} - a_s)/a_s|, \eta^{(i)}_b = |(b^{(i)} - b_s)/b_s|, \eta^{(i)}_d = |(d^{(i)} - d_s)/d_s|, \eta^{(i)}_e = |(e^{(i)} - e_s)/e_s|$ and $\eta^{(i)}_f = |(f^{(i)} - f_s)/f_s|$ ($i=1, 2$) represent the relative error of magnetic field gradients (a, b, d, e, f) in eight and ten single-axis magnetometers

configuration schemes, respectively. $\eta^{(i)}_X = |(X-X_s)/X_s|$, $\eta^{(i)}_Y = |(Y-Y_s)/Y_s|$ and $\eta^{(i)}_Z = |(Z-Z_s)/Z_s|$ ($i=1,2$) represent the relative error of vehicle position parameters in eight and ten single-axis magnetometers configuration schemes, respectively, where X , Y and Z are respectively the vehicle position parameters relative to the magnetic target calculated by equation (1).

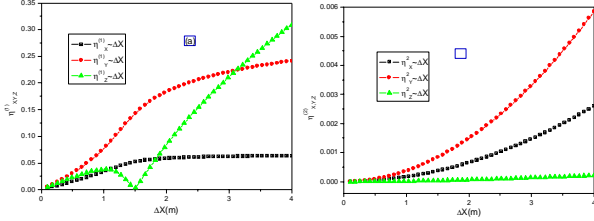


Fig.3 Curves between the relative error of calculated vehicle position parameters and ΔX

The curves between the relative error of magnetic field gradients and magnitude ($\eta^{(1)}_a, \eta^{(1)}_b, \eta^{(1)}_d, \eta^{(1)}_e, \eta^{(1)}_f, \eta^{(1)}_i$), ($\eta^{(2)}_a, \eta^{(2)}_b, \eta^{(2)}_d, \eta^{(2)}_e, \eta^{(2)}_f, \eta^{(2)}_i$) and the length of measurement line ΔX are shown in Fig.2 (a) and (b) and (c), respectively, when the range of ΔX is $0.1m \leq \Delta X \leq 10m$. From Fig.2, the relative error of magnetic field gradients and magnitude will increase with ΔX in two kinds of configuration schemes, but the relative error should increase rapider in eight single-axis magnetometers one. In other word, the relative error of magnetic field gradients in ten magnetometers configuration scheme is much smaller than in eight magnetometers one on condition of the same measurement line length. It is because, the connection lines of magnetometer teams with 7 and 8, 1 and 3, 1 and 6, 4 and 5, 2 and 7 all don't get across the measuring point P in eight magnetometers configuration, and their magnetic field differences aren't all related with magnetic field gradients of the point P . However, in ten magnetometers configuration, the connection lines of magnetometer teams with 1 and 4, 7 and 9, 2 and 5, 8 and 10, 3 and 6 all get across the measuring point P , so their magnetic field differences are all related with magnetic field gradients of the point P .

($\eta^{(1)}_X, \eta^{(1)}_Y, \eta^{(1)}_Z$), ($\eta^{(2)}_X, \eta^{(2)}_Y, \eta^{(2)}_Z$) and the length of measurement line ΔX are shown in Fig.3 (a) and (b), respectively, when the range of ΔX is $0.1m \leq \Delta X \leq 10m$. From Fig.3, the relative error will show a rise trend when ΔX lengthens in two kinds of configuration schemes, but the relative error should increase rapider in eight magnetometers one. In other word, the relative error of calculated vehicle position parameters in ten magnetometers configuration scheme is much smaller than in eight magnetometers one on condition of the same measurement line length. For example, $\eta^{(2)}_X, \eta^{(2)}_Y$ and $\eta^{(2)}_Z$ are only 1.12%, 0.83% and 0.08% of $\eta^{(1)}_X, \eta^{(1)}_Y$ and $\eta^{(1)}_Z$, respectively when $\Delta X=2m$.

From above analysis, we can know that the calculated error of target magnetic field magnitude and gradients is larger in eight magnetometers configuration although its cost is lower due to lack of two magnetometers, and the calculated error of vehicle position relative to the target is larger, too. So, the underwater localization precision based on magnetic anomaly is low. On contrary, the magnitude and gradients of target magnetic field can be calculated accurately in ten magnetometers configuration, and its localization error is small. And thus, ten single-axis magnetometers configuration scheme should be selected in the experiment of underwater magnetic field localization.

ACKNOWLEDGMENT

This work was supported by the National Nature Science Foundation of China under Grant Nos 60775001 and 60834005.

REFERENCES

- [1] Psiaki M L, "Autonomous orbit and magnetic field determination using magnetometer and star sensor data", *Journal of Guidance, Control, and Dynamics*, 18(3), pp.584-592, 1995.
- [2] Shorshi G, Bar-Itzhack I Y, "Satellite autonomous navigation based on magnetic field measurements", *Journal of Guidance, Control, and Dynamics*, 18(4), pp. 843-850, 1995.
- [3] Deutschmann J, Bar-Itzhack I Y, "Evaluation of attitude and orbit estimation using actual earth magnetic field data", *Journal of Guidance, Control and Dynamics*, 24(3), pp. 616-626, 2001.
- [4] Gao Changsheng, Jing Wuxing, Zhang Yan, "Autonomous navigation of low earth orbit satellites using magnetic measurements by unscented kalman filter", *Chinese Space Science and Technology*, 2, pp.27-32, 2006. (in Chinese)
- [5] Gao Jintian, An ZhenChang, GU ZuoWen et al. "Selections of the geomagnetic normal field and calculations of the geomagnetic anomalous field", *Chinese J. Geophys.*, 48 (1), pp.56-62, 2005. (in Chinese)
- [6] Hao Yanling, ZhaoYafeng, Hu Junfeng. "Preliminary analysis on the application of geomagnetic field matching in underwater vehicle navigation", *PROGRESS IN GEOPHYSIC*, 23(2), pp. 594 - 598, 2008. (in Chinese)
- [7] DonaldG Polvani, Arnold Md, "Magnetic marker position fixing system for underwater vehicles", Unite state patent: 5357437, 1982.
- [8] Arie Sheinker, Boaz Lerner, Nizan Salomonski et al, "Localization and magnetic moment estimation of a ferromagnetic target by simulated annealing", *Meas.Sci.Technol*, 18 ,pp. 3451-3457, 2007..
- [9] Tanekage Yoshii, "Method for detecting a magnetic source by measuring the magnetic field thereabout", Unite state patent: 4309659, 1982.